Gemi ve Deniz Teknolojisi Dergisi
Sayı: 221, Haziran 2022
ISSN: 1300-1973, e-ISSN: 2651-530X, Dergi ana sayfası: http://www.gmoshipmar.org/
Araştırma Makalesi

Açık Kaynaklı Panel Yöntemi Kodlarının Ticari Kod ile Karşılaştırılması ve Değerlendirilmesi

Muhammed Uçar [1,3], Emre Uzunoğlu [2], Elif Oğuz [3,4]

[1] Necmettin Erbakan Üniversitesi, İnşaat Mühendisliği Bölümü, Konya, Türkiye
[2] Deniz Teknolojisi ve Deniz Bilimleri Merkezi (CENTEC), Yüksek Teknik Enstitüsü, Lizbon Üniversitesi, Lizbon, Portekiz
[3] Hidrolik Laboratuvarı, İnşaat Mühendisliği Bölümü, Orta Doğu Teknik Üniversitesi, 06800, Ankara, Türkiye
[4] Rüzgar Enerjisi Araştırma Merkezi (METUWIND), Orta Doğu Teknik Üniversitesi, 06800, Ankara, Türkiye

[1] ucar.muhammed@metu.edu.tr, ORCID: 0000-0001-6062-7532
[2] emre.uzunoglu@centec.tecnico.ulisboa.pt, 0000-0001-6880-197X
[3,4] (sorumlu yazar), elifoguz@metu.edu.tr, 0000-0003-3574-9436

ÖZET

Bu çalışmada, iki yüzer rüzgâr türbini platformu üzerinden açık kaynaklı panel yöntemi kodlarına dair bir kıyaslama çalışması sunulmuştur. HAMS, NEMOH ve WAMIT; sonuçları, hesaplama performansları, kullanım kolaylıkları ve esneklikleri açısından karşılaştırılmıştır. OC3 Hywind Spar ve OC4 DeepCWind Semisubmersible yüzer platformları için WAMIT verileri önceki yayınlardan alınmış olup yapının hareketini temsil eden şu ana parametreler NEMOH ve HAMS değerleri ile karşılaştırılmıştır: yapıya etkiyen dalga kuvvetleri, katma kütle değerleri ve potansiyel sönüm değerleri. Her iki açık kaynak panel yöntemi kodu da, NRMS değerleri baz alınarak, çok elemanlı olan Semisubmersible platformdan ziyade, basit bir tek parça spar platform konseptinde daha başarılı olmuştur. Genel olarak, en yakın sonuçlar, katma kütle için ileri-geri öteleme yönünden; en olumsuz sonuçlar ise, dalıp-çıkma yönündeki radyasyon sönümlenmesinden elde edilmiştir. NEMOH, her iki platformda da baş-kıç vurmada uygun bulunamayacak sonuçlar vermiştir. NEMOH'un bu baş-kıç vurma sonuçları ihmal edilirse, her iki kod da WAMIT'e paralel ve makul derecede yakın sonuçlar vermiştir. Bu çalışmanın amacı, geçerliliği kabul edilmiş bir ticari koda alternatif olarak, araştırmacıların ücretsiz bir açık kaynak kodu seçebilmelerine yardımcı olmaktır.

Anahtar kelimeler: Panel Yöntemi, hidrodinamik katsayılar, açık kaynak, BEM çözücü, kıyaslama çalışması, açık deniz rüzgârı

Makale geçmişi: Geliş 20/04/2022 – Kabul 19/06/2022

https://doi.org/10.54926/gdt. 1106386

GMO Journal of Ship and Marine Technology
Issue: 221, June 2022
ISSN: 1300-1973, e-ISSN: 2651-530X, Journal homepage: http://www.gmoshipmar.org/
Research Article

Comparison and Evaluation of Open-Source Panel Method Codes against Commercial Codes

Muhammed Uçar [1,3], Emre Uzunoğlu [2], Elif Oğuz [3,4]

[1] Necmettin Erbakan University, Civil Engineering Department, Konya, Türkiye
[2] Centre for Marine Technology and Ocean Engineering (CENTEC), Instituto Superior Técnico, Universidade de Lisboa, Lisbon, Portugal
[3] Hydraulics Laboratory, Civil Engineering Department, Middle East Technical University, 06800, Türkiye
[4] Center for Wind Energy Research (METUWIND), Middle East Technical University, 06800 Ankara, Türkiye

[1] ucar.muhammed@metu.edu.tr, ORCID: 0000-0001-6062-7532
[2] emre.uzunoglu@centec.tecnico.ulisboa.pt, 0000-0001-6880-197X
[3,4] (corresponding author), elifoguz@metu.edu.tr, 0000-0003-3574-9436

ABSTRACT

This work provides a benchmark study regarding the open-source panel method codes of two floating wind turbine platforms. HAMS, NEMOH, and WAMIT are compared in terms of their results, computational performance, user-friendliness, and, flexibility. WAMIT's data is sourced from previous publications for the OC3 Hywind Spar and OC4 DeepCWind Semisubmersible. These reference values are compared to NEMOH and HAMS for the main parameters representing the movement of the structure: wave excitation forces, added mass values, and potential damping. Both of the open source panel method codes were quite successful in the concept of a simple one-piece spar float rather than a multibody semi-submersible in terms of NRMS values. Overall, the most close results were obtained from the surge for added mass, and the most unfavorable results were from radiation damping in the heave. NEMOH brings ineligible results for pitch on both platforms. Neglecting the pitch axis results of NEMOH, both codes showed parallel and reasonably close results to WAMIT. The study aims to help researchers to choose a free open-source alternative to a validated commercial code.

Keywords: Panel Method, hydrodynamic coefficients, open-source, BEM solver, benchmark study, offshore wind

Article history: Received 20/04/2022 – Accepted 19/06/2022

ISSN: 1300-1973, e-ISSN: 2651-530X, Dergi ana sayfası: http://www.gmoshipmar.org/
Araştırma Makalesi

1. Introduction

One of the most known and preferred renewable energy sources today is wind energy. However, it is difficult to install and operate wind turbines on land due to noise and visual pollution and insufficient space to install them on land. Compared to the land, there are much higher wind speeds and therefore higher energy potential per square meter on the coasts and the deeper seas as you move away from the coast. To realize this potential, there is a trend toward the Floating Wind Turbines (FWTs) (Shin et al., 2013), and the vision of FWTs was first proposed by Professor William E. Heronemus (1972) at the University of Massachusetts. After the commercial wind industry was well established, the issue was again taken up by the research community. The economic potential of FWTs was demonstrated by Musial et al. (2004).

The cost of onshore wind power today is competitive with most fossil fuels and will likely be cheaper than the new "clean" coal (Andersen et al., 2015). Three main factors play a key role in this success: 1) dramatic reductions in turbine costs, 2) increased reliability, and 3) economy of scale in production. The first two developments were the result of improvements in design techniques and design tools. Aerodynamic research was followed by aero-elastic dynamic models, and finally, the standards were developed as a result of extensive research (Andersen et al., 2015). Offshore wind energy resource is 50% higher than onshore; however, the cost of installing and operating offshore wind power units is about twice that of onshore (IRENA, 2012). On the other hand, cost reduction studies are ongoing for also platform and mooring costs (especially Tension Leg Platform (TLP)) costs. As an example, Compos et al. (2016) compared the costs of steel and an equivalent concrete spar buoy and revealed that the concrete monolithic design was 60% cheaper in terms of material costs. While the wind industry and researchers agree on the higher cost of offshore wind power, many argue that offshore wind power is cost-competitive with land-based fossil fuel production when environmental impacts are added to the cost equation (Butterfield et al., 2007). Offshore wind power generation is mainly located in areas 5−50 km from the shoreline, where the water depth is usually more than 20 m. Studies have shown that conventional fixed foundations will not be economically viable in waters deeper than 30 m (Andersen et al., 2015). Coasts with a narrow coastal shelf, such as the coasts of the United States, China, Japan, Spain, Portugal, and Norway, are an example. Mounting wind turbines on floating support structures opens up the potential to exploit such deepwater resources. To use such deep water sources, wind turbines must be mounted on floating support structures (Cordle and Jonkman, 2011). Fortunately, the long-term survivability of floating structures has been successfully demonstrated for decades by the marine and offshore oil industries (Butterfield et al., 2007).

Floating offshore wind turbine platforms are classified into three main types, spar-buoys, TLPs, and semi-submersibles, and can be stabilized by mechanical means such as deep ballast placement (e.g., a SPAR), mooring line tension (e.g., a TLP), or the waterplane area (e.g., a barge), all platforms use a combination of these methods. Each one of these methods has their advantage and disadvantages depending on site conditions and placement methods in that they are cost-driven in size, complexity and flexibility (Olondriz et al., 2016). Butterfield et al. (2007) presented design challenge trade-offs for stability criteria with a framework for the classification of floating wind turbine platforms to perform first-order economic analysis on a wide variety of platform architectures based on static stability criteria. His classification was subsequently updated by several authors to clarify the primary contributor (Uzunoglu and Guedes Soares, 2020).

In terms of design and analysis, the dynamic behaviour of a structure in water is directly relevant to many technologies, including vessels, offshore platforms, and wave energy converters (WECs). Comprehensive simulation codes are needed to design and analyse coupled dynamics of offshore wind

turbines that take into account aerodynamics, hydrodynamics, mooring dynamics, foundation dynamics, elasticity, fatigue, and combined dynamics of turbine controls (Robertson et al., 2014). Matha et al. described the major modelling challenges, development needs, and advanced modelling methods developed to meet these needs for floating wind turbine codes (Matha et al., 2011). Various numerical methods have been developed to model such a system, from high-fidelity Navier-Stokes computational fluid dynamics (CFD) codes, which model the fluid-structure interactions from first principles, to moderately accurate potential flow time-domain models and simple frequency-domain methods (Lawson et al., 2015). Matha et al. discuss the limits of potential flow methods and Boundary Element Method (BEM) and the competencies of CFD for FWT simulation (Matha et al., 2011). A comparison between a viscose time domain and a CFD model was made by Bhinder et al. (2015) and a methodology for describing and incorporating the drag damping force in potential flow-based models is presented and shown to be in reasonable agreement with CFD simulations (Bhinder et al., 2015). While frequency domain methods continue to be widely used in the offshore oil and gas industries to analyse and design floating structures, these methods are also used for the preliminary design of floating wind turbines. Henderson et al. (2003) utilized linear frequency-domain hydrodynamic techniques to analyse a tri-floater concept and find response amplitude operators (RAOs). Lee (2005) conducted a similar process to investigate a TLP design. Vijay et al. (2016) also used frequency domain analysis to evaluate the motions of a barge with a central moonpool that combines a wave energy converter with a 5-MW turbine. Wayman et al. (2006) modelled various barge and TLP designs in the frequency domain. Sclavounos et al. (2008) conducted a parametric design study for FWT concepts and mooring systems based on coupled linear dynamic analysis in the frequency domain. Potential flow solutions have also been integrated into the system, showing their applicability for initial design purposes (Uzunoglu and Guedes Soares, 2019).

International Energy Agency Wind Tasks 23 and 30, the Offshore Code Comparison Collaboration (OC3) and Offshore Code Comparison Collaboration Continuation (OC4) studies were carried out to evaluate offshore wind turbine modelling tools through code-to-code comparisons. These projects have been successful in demonstrating the effect of different modelling approaches on the simulated responses. These code-to-code comparisons were used only to identify differences, while scale hydrodynamic tank testing was performed in the Dutch Maritime Research Institute's offshore wave basin for data validation and published within the OC5 project as a continuation (Uzunoglu and Guedes Soares, 2019). Several FWT analysis tools were used in OC4, including FAST, ADAMS, Bladed, HAWC2, 3Dfloat, SIMO, SESAM, and DeepC. Various loading conditions were compared in the models. These included a full-system Eigen analysis; a static equilibrium test; free decay tests for each of the platform's six degrees of freedom; “effective RAOs” calculated with regular waves of varying frequencies; Time series response tests with regular waves and irregular waves modelled with rigid rotor under no-wind as well as flexible rotor under steady and turbulent wind (Cordle and Jonkman, 2011). In another study, results from InWave-CACTUS were compared with results from FAST for OC3 Hywind Spar (Robertson et al., 2017). The InWave-CACTUS method showed good agreement with the FAST results for small-amplitude motions (Jonkman et al., 2010). CACTUS (Murray and Barone, 2011) is a lifting-line free vortex wake method implemented at Sandia National Laboratories (SNL) (USA). A modular framework, CACTUS is coupled to InWave (Combourieu et al., 2014; Leroy et al., 2017), a maritime code developed at INNOSEA (Nantes, France) in collaboration with the LHEEA Laboratory of Ecole Centrale de Nantes, integrated with the linear potential flow solver NEMOH.

Coupled dynamic codes developed for modelling FWT platforms include one of two hydrodynamic models: (1) Morison's equation (Morison et al., 1950), or (2) potential flow theory which may also

include the nonlinear viscous drag term from Morison's equation (Robertson et al., 2017). Details of Morison's equation and Potential flow theory are given in section 2.1.

The offshore platforms located on deepwater sites and the most frequently referenced (Penalba et al., 2017) potential flow code WAMIT has long been used in numerous studies for offshore platforms. Parisella and Gourlay (2016) compared and showed that the excitation forces, hydrodynamic coefficients and RAOs are in good agreement for a cargo ship in shallow water between NEMOH and WAMIT results through different conditions and cases. The world's first open-source and widely used potential flow code (Penalba et al., 2017) released in 2014, NEMOH, has also gained some confidence and has been used in a variety of case types in different fields such as; WECs (Lawson et al., 2015; Verbrugghe et al., 2017; Fernandez et al., 2018; Bhinder & Murphy, 2019; Schubert et al., 2020), FWTs (Antonutti et al., 2016; Zhou et al., 2019; Jonkman et al., 2010), Hybrid wind-wave energy platforms (Kohlmann, 2019; Armesto et al., 2016; Gonzalez Jimenez, 2020) and breakwaters (Doss, 2020).

Roessling and Ringwood stated that for a simple vertical cylinder, the codes WAMIT, NEMOH and Achil3D show a very good match for heave. However, compared to WAMIT, NEMOH has the disadvantage of requiring longer computation times (Roessling & Ringwood, 2014). Bhinder and Murphy (2019) compared the three radiation-diffraction panel codes (WAMIT, AQWA and NEMOH) with the experimental results and stated that the results showed a very good agreement for the calculated frequency domain parameters. In this comparison, simulations are made for an irregular (panchromatic) wave using a nonlinear time-domain model. Experimental data and statistical measurements of BEM codes such as correlation coefficient and root mean squared error (RMSE) showed very good results. The authors implied that the nonlinear properties of wave structure interactions can be considered through additional nonlinear viscous drift damping in accordance with Morison's equation (Bhinder & Murphy, 2019). Penalba et al. (2017) compared the results of NEMOH and WAMIT on the added mass, radiation damping and excitation force coefficients added by a WEC and noted that they were consistent with some exceptions. The exceptions include thin element modelling and irregular frequency removal, which expresses uncharacteristic high amplitudes of some frequency components. However, this only affects results in low wave periods, which produces a negligible effect on a FOWT structure (Hughes et al., 2020). Andersson (2018), investigated the reliability of the NEMOH program in his master's thesis on the cases of three container ships. He noted that the results from NEMOH showed positive agreement with WAMIT overall, but with a small shift in amplitudes for pitch. The author stated that the heave and pitch RAO results of NEMOH corresponded well to the WAMIT data while noting that the additional mass and damping coefficients found for heave were overestimated for the same frequency range. Andersson also emphasized the low accuracy of NEMOH in low wave periods. The author questioned whether the reason for the divergent results he found was insufficient input by the authors or a lack of robustness in the NEMOH, and referenced a comparison study (Kim, Y. & Kim, J.-H, 2016), in which ten participants and seventeen-code is compared. As a result, the author reflects that NEMOH cannot be fully compared with the accuracy and robustness of WAMIT (Andersson, 2018).

WAMIT is the most frequently referenced, widely used and validated BEM code for estimating the hydrodynamic behaviour of offshore structures. However, the code is commercial limiting its reach. Two alternative codes can be considered by the research community. Both are open-source; therefore, they can also be developed further. The world's first open-source and widely used BEM code (Penalba et al., 2017), NEMOH, was released in 2014. Several publications have compared its results to WAMIT as mentioned above. Additionally, HAMS is a recently released (Liu et al., 2018; Liu, 2019; Liu, 2021) open-source BEM code that can now be included in benchmark studies to evaluate its output. This

study aims to present the data that serves to present open-source alternatives that serve to obtain the hydrodynamic coefficients.

The paper is structured from here on as follows. The methodology section includes brief explanations for the theories and the codes for the estimation of the structural loads and responses. Then the modelling section introduces the chosen structures and conditions that the comparison is made upon. The mesh study section follows the modelling section and followed by the main study section that discusses the abilities of the open-sourced BEM solvers. The study results in a with a brief conclusion section.

2. Methodology

2.1. Prediction of hydrodynamic loads for offshore structures

2.1.1. Flow regimes

Calculation of wave forces acting on offshore structures can be divided into different basic procedures, depending on the size of the structural element and the wavelength and height of the incoming waves. Morison's equation (Zhao et al., 2019) is used to estimate the forces resulting from wave behaviour, assuming that the diameter of the element is sufficiently small compared to the wavelength (limited by $D/\lambda<0.2$) so as not to significantly change the wave characteristics. The Morison equation is based on the assumption that the waves are not affected by the presence of the submerged members. Conversely, in nature, incoming waves are reflected from the object (wave diffraction) and the object sends waves due to its movement (wave radiation). If the object is larger than the corresponding wavelength, these two effects become more relevant and act as dispersive forces. Morrison's equation, diffraction and radiation damping effects are omitted, flow separation effect is partly accounted for in the viscous drag term (Chakrabarti, 1987). Besides, for larger structural elements (with $D/\lambda>0.2$), diffraction theories are required to take into consideration the radiation and diffraction as well (Figure 1). However, these potential flow methods cannot take into account viscous drag forces (van der Tempel et al., 2011). Secondly, the H/D parameter is essential because, in an oscillatory wave flow, the drag forces on the structures (as in the example of a circular tube) affect the flow separation behind the cylinder and thus the formation of large eddies. For a small H/D ratio (<1.5), the relative displacements of the water particles are so small and the wave height is not unidirectional long enough that the water around the structures remains attached to the surface of the structure and the phenomenon of flow separation and eddy development caused by diffraction is not observed, so the viscous effect can be ignored (Figure 1) (Fitzgerald, 2016). In these conditions, the drag forces are very small and the dominant forces are the inertial forces due to acceleration, so the potential flow diffraction theory should be used to predict wave forces. For H/D> 8, approximately, the Morison formulation is required to be used, since the wave flow is unidirectional long enough for a significant eddy flow to develop, and the drag forces are greater. It has been stated that in an intermediate region with $1.5 < H/D < 8$, the flow regime can be quite complex and it is difficult to calculate wave forces (van der Tempel et al., 2011).

2.1.2. The Morison equation

The Morison equation introduced by Morison O'Brien Johnson and Schaaf (Morison et al., 1950) is a semi-empirical equation describing the horizontal hydrodynamic forces acting on a body along the direction of incoming waves. To compute hydrodynamic forces, the equation requires two empirical

ISSN: 1300-1973, e-ISSN: 2651-530X, Dergi ana sayfası: http://www.gmoshipmar.org/
Araştırma Makalesi

coefficients (inertia and drag), the water particle velocities and accelerations and, the geometry of the structure. Three components are combined in the equation: the first term is the “Froude-Krylov force” term which is due to the pressure field generated by the undisturbed waves. The second term is the so-called “added mass” term which is due to the inertia of the surrounding fluid that needs to be accelerated. And the last term is the drag term which is due to the wake region on the "downstream" side of the cylinder (Patel, 1994; Fang & Duan, 2014). For a submerged cylindrical body, the Morison equation can be described with an infinitesimal strip ds as

$$dF = \rho \pi D^2/_4 \frac{du}{dt} ds + C_A \rho \pi D^2/_4 \left(\frac{du}{dt} - \frac{du_b}{dt}\right) ds + C_D \rho (u - u_b)|u - u_b|/_2 D ds \quad (1)$$

dF is the total fluid force, ρ is the fluid density, D is the cylinder diameter, u is the fluid velocity, u_b is the velocity of the body, C_A is the added mass coefficient, and C_D is the drag coefficient. By summation of the first and second term, one can obtain the inertia term, and $1 + C_A = C_M$, while C_M is the inertia coefficient. C_A , and C_D is investigated by experimental analysis, and the empirical relations for the coefficients are determined accordingly. The case studies of this paper have large-diameter submerged members, hence the Morison equation is not utilized in this study. Instead, diffraction theory-based potential flow solvers are used and compared with each other.

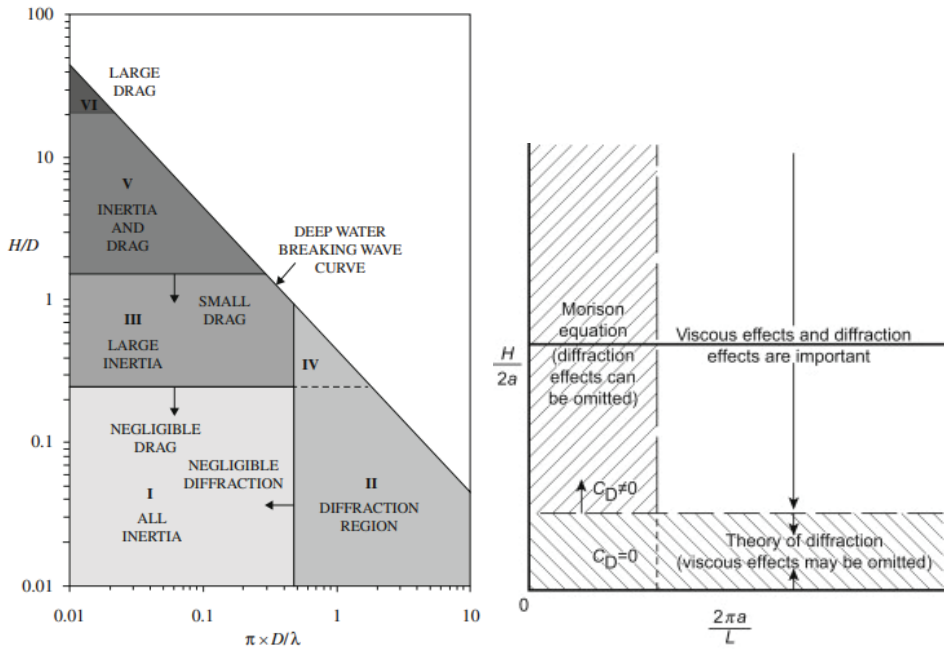

Figure 1. Flow regimes and applicability regions of the theories, D=2a (Fitzgerald, 2016; Wang et al., 2020)

2.1.3. Diffraction Theory-Potential flow approach

In the potential flow theory, it is assumed that the interactions between ocean waves and marine structures occur in a regime where compressibility and viscous effects are negligible, that is, water behaves like an ideal fluid. In offshore engineering, the incompressibility assumption is standard (because of the encountered low speeds); however, viscous effects can play an important role depending on the wavelengths, wave amplitudes, and, flow regime compared with the body size. Flow separation is confined around any sharp corner and might be neglected for large structures with relatively small movements, such as offshore platforms, especially in the preliminary design phase.

Thus, the boundary layers are comparatively thin and therefore the drag and viscous forces are substantially smaller than the corresponding potential flow forces (WAMIT User Manual, 2006). The potential theory is based on the potential function ϕ, gradient (∇) of the potential function is velocity field $\nabla\phi = \vec{V}$. Due to the definition of irrotational flow $\nabla \times \vec{V} = 0$, ϕ must satisfy the Laplace equation $\nabla^2\phi = \vec{V}$.

$$\partial^2\phi/_{\partial x^2} + \partial^2\phi/_{\partial y^2} + \partial^2\phi/_{\partial z^2} = 0 \quad (2)$$

Boundary value problems arise for the solution of this equation. The bottom and the free surface are required to be solved with dynamic and kinematic boundary conditions. At the bottom, the normal velocity component to the bottom must always be zero. And for the free surface, fluid particles must remain on the surface and free surface pressure must be equal to atmospheric pressure (Babarit & Delhommeau, 2015). Panel methods are popular in hydrodynamics where the floating bodies are discretized into many surface elements (i.e. panels) to solve the boundary conditions on the immersed body. To obtain the velocity potential, ϕ, the problem is transferred to a set of algebraic equations, which are structured by placing a distribution of vortices, sources and/or doublets on the surface elements (panels) with proper boundary conditions. The velocity potential is assumed to be in the form of $\phi = \phi_0(z)\sin(kx - \omega t)$, so the resulting force is also periodic with the frequency ω. Therefore, time-dependent problems with random wave patterns are not suitable to be solved with potential theory approaches (Patel, 1994). Once the velocity potential is solved, the pressures and hence the loads affecting the structure can be calculated by Bernoulli's equation:

$$\partial\phi/_{\partial t} + \frac{1}{2}\nabla\phi.\nabla\phi + p - p_a/_{\rho} + gz = 0 \quad (3)$$

2.2. Potential flow solvers

The comparison study made in this paper is based on the potential flow theory and the potential flow solvers. The solvers are developed to analyse the behaviour of offshore structures interacting with surface waves. As explained in the previous section, fluid is assumed to be ideal and the flow is assumed to be periodic. The free surface state is linearized. Diffraction and radiation velocity potentials at the submerged body surface are determined by the solution of an integral equation derived from Green's theorem (Liu, 2019).

Table 1. BEM Solvers and their Characteristics after (Penalba et al., 2017)

BEM solver	Frequency domain	Time-domain	Open source	Usage (%)
WAMIT	+	-	-	80.5
NEMOH	+	-	+	19.5
AQWA	+	-	-	22.0
Aquaplus	+	-	-	9.8
ACHIL3D	-	+	-	4.9
WADAM	+	-	-	7.3
HAMS	+	-	+	NA

HAMS is released in 2021 (Liu, 2021), therefore its usage rate is not included in the table (Penalba et al., 2017). WAMIT was cited in more than 80% of articles referring to a BEM solver, and it was the most frequently referenced BEM code. Therefore, WAMIT can be regarded as the de-facto standard. The reason why WAMIT is taken as the benchmark for NEMOH and HAMS in this study is the common use

ISSN: 1300-1973, e-ISSN: 2651-530X, Dergi ana sayfası: http://www.gmoshipmar.org/
Araştırma Makalesi

of WAMIT by the oil, gas, wave and wind energy community. WAMIT, NEMOH, and HAMS consist of three main procedures designed to work sequentially: pre-processor, processor, and post-processor. WAMIT offers an inclusive user manual that explains each required input file and option of the software, together with all the outputs generated; NEMOH and HAMS only provide a brief explanation of the code with limited instructions for using the software. Parallel processing is available for every BEM code (WAMIT User Manual, 2006; Liu, 2019).

2.2.1. WAMIT

WAMIT is a FORTRAN-based BEM code that offers two fundamentally different methods of geometry discretization: low and high order. The standard discretization method is the low order method in which the geometry of the object is divided into many flat quadrilateral panels. The high-order method provides the advantage of including curvature. WAMIT provides 2 symmetry planes (y0z and x0z), which can reduce the computation time. WAMIT requires a proprietary geometric format (<file>.gdf extension) for mesh files, and very few software can export it. Thus, WAMIT users can either use predefined subroutines for simple geometries or certain software such as Rhinoceros or MultiSurf to create their meshes. Since WAMIT produces dimensionless results, parameters such as seawater density or gravity are not required for WAMIT (WAMIT User Manual, 2006). To simulate WAMIT, at least five input files are needed. Mesh geometry file, with .gdf extension, defines the wet surface of the body to be analysed. Config.wam and SIM.cfg specifies many parameters and options including mesh and parallelization. SIM.pot calls the mesh file and defines the environmental parameters and the body-fixed coordinate system. SIM.frc contains body information such as stiffness and mass matrices and flags for output results (WAMIT User Manual, 2006).

2.2.2. NEMOH

NEMOH is a FORTRAN-based BEM code that requires at least four input files for simulation. One of them is the ID.dat file which is a simple file identifying the name of the simulation. Another one is the input.txt file containing solver selection. All the parameters needed for NEMOH simulation are in a single input file named NEMOH.cal. The last input file required by NEMOH is a mesh file. NEMOH users can use the two MATLAB functions, axially symmetrical (axiMesh.m) and non-axial symmetrical (Mesh.m), to create their meshes. Additionally, NEMOH includes the GDFmesh.m function, which directly reads .gdf meshes, a WAMIT extension. It also offers the NEMOH2WAMIT_01.m function, which converts NEMOH mesh files to .gdf format. NEMOH, geometries are limited to 10000 nodes or 2000 panels, whether they are created with their sub-functions or .gdf files. NEMOH offers only the low-order geometry discretization method and the result is quite similar to the low-order mesh created in WAMIT. NEMOH allows only one plane of symmetry (x0z). NEMOH provides a MATLAB wrapper (NEMOH.m) to run simulations, making the process user-friendly for users familiar with MATLAB (Penalba et al., 2017).

2.2.3. HAMS

HAMS (Hydrodynamic Analysis of Marine Structures) is written currently in FORTRAN 90 (Liu, 2019). HAMS has no mesh generator inside, instead, the mesh is imported. HAMS offers two symmetry planes, whereas only offers the low-order geometry discretization method. WAMIT's .gdf format is required to define the mesh in the first step. Then it is necessary to use the built-in tool WAMIT_MeshTran.exe to convert the .gdf mesh to HAMS mesh formats such as WaterplaneMesh.pnl

and HullMesh.pnl. HAMS requires two additional input files besides these two mesh files. One of them is ControlFile.in, which is the main input control file containing all the necessary parameters. Finally, the Hydrostatic.in file also needs to be filled in for RAO calculations, yet the necessary information can be obtained from the fort.4 file created by WAMIT_MeshTran.exe (Liu, 2021).

2.3. Equations of motion

For hydrodynamic predictions, a floating body can be considered mostly rigid but moving. A floating body of arbitrary form can present hydrodynamic reactions caused by motion in any *j* direction at all six degrees of freedom (DOF), *i*. In the case of a simple monochrome incident wave, the equations may look like this:

$$\sum_{j=1}^{6}[(A_{ij}+M_{ij})\ddot{\eta}_j + B_{ij}\dot{\eta}_j + C_{ij}\eta_j] = \sum F_i \text{ for } i=1\ldots 6 \quad (4)$$

where η is the position of the body, A_{ij} is the hydrodynamic added mass matrix elements, M_{ij} is the generalized mass matrix elements, B_{ij} is the radiation damping or hydrodynamic damping coefficients, C_{ij} is the restoring or hydrostatic stiffness coefficients, and $\sum F_i$ represents the sum of all other forces in the direction of *i* that may be present. A dot on a symbol indicates a derivation of time. Hydrodynamic properties and radiation damping are the functions of the frequency of motion and Equation (4) needs to be solved for excitation as a harmonic function. The first term, $(A_{ij}+M_{ij})\ddot{\eta}_j$, the inertia of mass is increased by a hydrodynamic "added mass"; because, to accelerate the body, it is also needed to accelerate the water surrounding it. The added mass for submerged objects near the water surface may be negative but is always positive for objects submerged deeply (Bergdahl, 2009). Potential flow approaches are characteristically applied within the frequency domain, and this is essential for determining the RAO. RAO is a frequency-dependent factor and represents the ratio of the floating platform's response (output) based on a regular wave signal (input) (Patel, 1994).

$$RAO(w) = {F_0}\Big/{(C-(M+A(w))w^2 + iB(w)w)} \quad (5)$$

3. Modelling

In this study, two of a few well-known structures are chosen to compare potential flow codes. The structures are already verified experimentally and computationally and the structures have different stabilization principles, which is highly important for the code compatibility regarding whether the codes are biased to any stabilization behaviour or excess movement. One is mainly stabilised with ballast-gravity and the other is mainly stabilized with the waterplane area-bouyancy. One of them is a Spar-Buoy concept called "Hywind" developed by Statoil from Norway. The original design was slightly modified by the OC3 to support the National Renewable Energy Laboratory's (NREL) 5 MW base turbine. The current version was named "OC3-Hywind" and was used for the benchmark study of OC3. The other structure is a semi-submersible concept used in the DeepCWind project. DeepCWind is a US-based project that aims to generate test data for use in the verification of FWT modelling tools. NREL's 5 MW base turbine is also used in DeepCWind Semi-Submersible for benchmarking of OC4, a Continuation project of OC3. The same geometry files are drawn in Rhinoceros and used in the compared codes. Mesh effect and independence studies are carried out for NEMOH and HAMS only because there was no commercial license for WAMIT. WAMIT meshes and results are obtained from HydroDyn sample input files for the final versions used in OC3-OC4 projects and distributed freely with FAST (Jonkman, 2005).

ISSN: 1300-1973, e-ISSN: 2651-530X, Dergi ana sayfası: http://www.gmoshipmar.org/
Araştırma Makalesi

3.1. OC3 Hywind Spar-Buoy

The stabilization method of the platform is predominantly ballast type, with high inertial resistance and righting moment thanks to the lower centre of mass. The NREL 5-MW baseline wind turbine tower on top of the OC3-Hywind spar-buoy is erected on a base diameter of 6.5 m, matching the top diameter of the platform. The resulting total tower mass is 249,718 kg and the tower centre of mass (CM) is located at 43.4 m on the tower centreline above the SWL. The critical structural damping rate of 1% was determined for all modes of the isolated tower. The platform consists of two cylindrical zones connected by a linearly tapered conical zone, the diameters of these cylinders are 6.5 meters and 9.4 meters. With this design, the hydrodynamic loads are reduced by using a smaller diameter near the free surface. The 6.5 m diameter cylinder zone extends up to 4 meters under SWL, while the conical zone is 8 meters long vertically. The weight of the floating platform is 7,466,330 kg including ballast. The CM of this mass is located at 89.9155 meters below the SWL along the platform centreline. The floating platform's roll and pitch inertias around CM are both 4.229.230.000 kg.m2 and the yaw inertia around the centreline is 164.230.000 kg.m2. For stabilization, the platform is connected by three catenary lines spread symmetrically around the centreline (Jonkman, 2010).

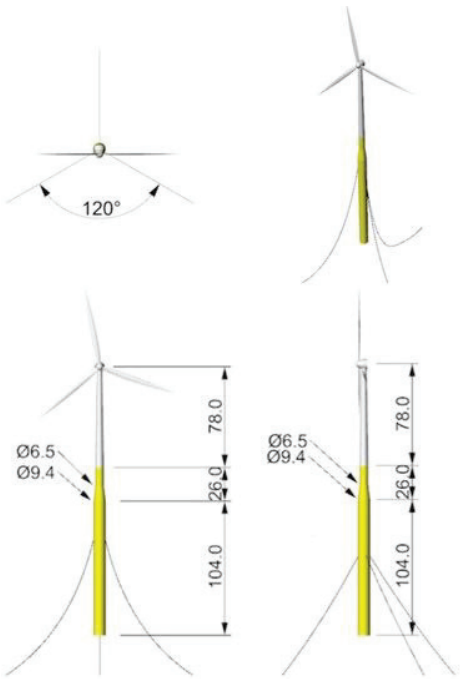

Figure 2. The schematic diagrams of the OC3-Hywind spar with the catenary mooring lines in different views after (Lin et al., 2019).

3.2. OC4 DeepCWind Semisubmersible

The stabilization method of the platform is predominantly buoyancy and ballast, rotational displacements caused by environmental conditions induce large lifting-restoring forces thanks to displaced water volumes. The tower used in the OC4 DeepCWind semi-submersible is almost the same as the OC3-Hywind spar-buoy tower. The only difference is the tower mode shapes caused by changes in the support platform and mooring. The DeepCWind semi-submersible platform consists of a main column on which the tower is mounted, and three offset columns connected to the main column by a series of smaller diameter pontoons and cross members. All three offset columns have larger diameter base columns at the base that helps suppress movement (especially in the direction of heave). The mass of the floating platform including ballast is 1.3473E + 7 kg. The CM of this mass is located at 13.46

m below the SWL along the platform centreline. The floating platform's roll and pitch inertias around the CM are both 6.827E + 9 kg.m2 and the yaw inertia around the centreline is 1.226E + 10 kg.m2. To stabilize the platform, moorings are spread out as on the OC3 Hywind Spar-Buoy (Robertson et al., 2014).

3.3. Environmental conditions and solver settings

Gravitational acceleration and seawater density were taken as 9.80665 m/s² and 1025 kg/m³, respectively. The water depths for OC3-Hywind Spar-Buoy and Semi-Submersible are 320 m and 200 m under SWL respectively. Effects of moorings were not taken into account and only the 0-degree incident waves are represented for NEMOH and HAMS. All calculations were done for six degrees of freedom. Wave periods were simulated from 2 seconds to 25 seconds. This range is preferred because the high response of floating structures to wave effects is observed within this range (Uzunoglu & Guedes Soares, 2020).

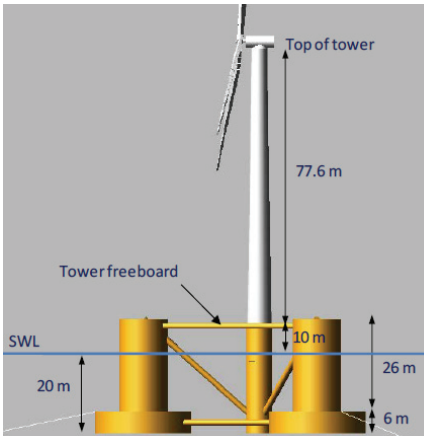

Figure 3. The schematic diagram of the DeepCWind Semi-Submersible (Robertson et al., 2014).

4. Effects of mesh on potential flow solution

For the potential flow solution, DNV suggests a mesh size using 1/6 of the smaller wave frequency of interest, which corresponds to an average panel side length of 4.6 m. It is also stated in the same document that the mesh size must be small enough to accurately represent the geometry. When the platform volume is compared to a mesh size reference of m3, m4 meshes result in an acceptable volume difference of less than 0.5 percent for both of the structures. This value is compatible with similar studies on panel methods in which geometry should be discretized (Uzunoglu and Guedes Soares, 2020; Jafaryeganeh et al., 2014; Ko et al., 2011). For OC3 Spar Buoy, however, the panel number limitation of NEMOH by 2000 is already reached with m4. Accordingly, an average side length of 1 m mesh is used for the OC3 Hywind Spar Buoy platform and an average side length of 1.5 m mesh is used for the OC4 DeepCWind Semisubmersible platform for potential flow code comparisons with m4 named meshes. However, the effect of mesh intensity is studied below.

Using a larger mesh reduces the number of elements and provides a faster solution, but also affects the accuracy of the results. On the other hand, using finer mesh significantly increases processing time and becomes less important after convergence. Therefore, a trade-off between the acceptable accuracy and the reasonable processing time is required. Although faster solutions are obtained in

potential flow codes compared to CFD studies, it is still important to perform mesh independence studies to maintain the trade-off. In this context, by conducting a study on mesh convergence, the sensitivity of the results to mesh shape and size is examined. The mesh sensitivity is only studied for the open-source codes. Wamit output is received from published sources.

Four meshes and their volumetric and time cost properties are studied for OC3 Hywind Spar-Buoy. The same study is conducted for OC4 DeepCWind Semisubmersible with a difference, the bracings are not included for mesh studies. The effect of bracings on this platform is studied by Uzunoglu and Guedes Soares (Uzunoglu & Guedes Soares, 2015) under different loading conditions, the authors showed that the bracings can be omitted at the preliminary design phases due to the negligible influence on the overall hydrodynamic behaviour. Thus, the bracings are neither included in the mesh study nor included in the calculation of normalized volume 100*(Vmesh-Vsimple design)/Vsimple design. So the increase in panel number due to the inclusion of these bracings increases simulation time cost for both codes but does not affect volumetric representation for the last data of OC4 DeepCWind Semisubmersible that has maximum panel number.

Normalized volume is used for non-dimensional geometrical representations of two platform systems relative to panel numbers. For the lowest panel numbers, only about 90% of the geometry is represented, because the discretized representation of cylindrical shape members in the Cartesian coordinate system needs more faces for polygonal prisms. With the increase in prism faces, the geometrical representation gets better rapidly at a certain point, after that, the increase in panel number becomes less and less effective. As shown in Figure 4, the lines indicating normalized volume values become almost flattened, and the final meshes provide about 99% normalized volume values.

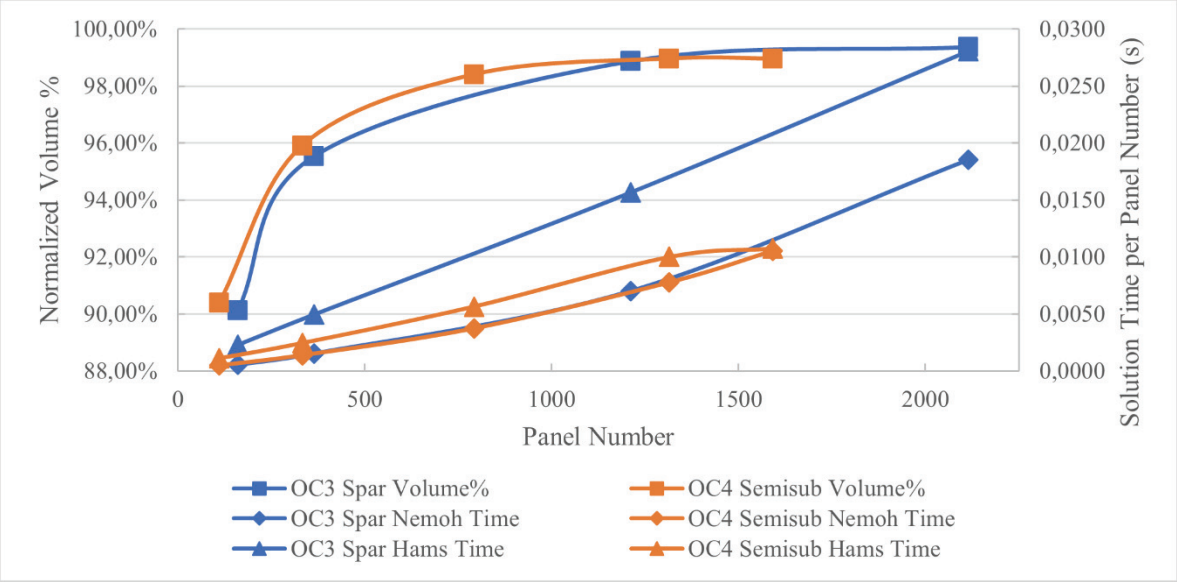

Figure 4. Variation of simulation time cost per panel number and geometrical representation with panel number

On the other hand, solution time per panel number and wave period is used to show the variation of code performances relative to panel numbers. To make a comparison, the processor used in simulations is a 12-core i7-8700K CPU @ 3.70 GHz. To conduct a parallel process, HAMS uses all the cores of the processor without any settings requirements; however, one may increase the OpenMP thread number to a certain limit (WAMIT User Manual, 2006) to enhance the performance. On the other hand, NEMOH needs modification as using “parfor” loops instead of “for” loops (Andersson,

2018) for parallelization in executable files, and thus in source codes, not implemented in this study. For the same amount of wave periods, simulation time cost per panel number always increases with an increasing number of panels almost linearly except the bracing included mesh for semisubmersible platform. For the same platforms, HAMS needs more simulation time to simulate the same geometry and wave periods even with using parallel processing compared to NEMOH.

Instead of representing the distribution of Added Mass (A), Radiation Damping (B) and Excitation Forces (Fe) in each period in a separate graph, the mesh convergence of both floating platforms is decided to be represented with normalized root mean square error (NRMSE) values with increasing panel numbers. While any floating object has six degrees of freedom, only the NRMSE values for surge, heave and pitch axis are represented here. This is due to the symmetrical shapes of the floating bodies, i.e. the effect of 0-degree incident waves is negligible for roll, sway and yaw.

The same meshes are used in both potential flow solvers and the exact panel number of meshes can be read from Table 2, However, the convergence of the results is not close to each other for both floating platforms. As mentioned previously, there is a trade-off between accuracy and time cost in terms of mesh size, this is also observed in this study with a few exceptions which are within an acceptable limit of numerical errors.

Table 2. The data of compared meshes

Meshes	Normalized Volume (%)	Panel Number	Simulation Time(s) / Panel # / period #	
			NEMOH	HAMS
m1_OC3_Spar	90.12	160	0.0005	0.0023
m2_OC3_Spar	95.53	364	0.0015	0.0049
m3_OC3_Spar	98.87	1212	0.0070	0.0157
m4_OC3_Spar	99.36	2115	0.0185	0.0280
m1_OC4_Semisub	90.38	111	0.0005	0.0011
m2_OC4_Semisub	95.91	333	0.0014	0.0024
m3_OC4_Semisub	98.41	792	0.0037	0.0056
m4_OC4_Semisub	98.96	1314	0.0078	0.0100
m4_OC4_Semisub+bracings	98.96	1569	0.0107	0.0109

Comparing the results of both potential flow solvers for the OC3 Spar Buoy platform, the most similar results are obtained for Excitation Force values in each surge, heave and pitch axis. Yet, these results are already within an acceptable limit provided by the coarsest mesh m1_OC3_Spar under 5% except heave axis Fe value in NEMOH. This implies that the Excitation Force accuracy is not highly dependent on the mesh size for such a simple geometry in the studied frequency range. Both codes produced the worst convergence results in radiation damping values in the heave axis, this can be explained by the waterplane area dependence of this value. Other than radiation damping in the heave axis, all of the data for m3_OC3_Spar have an NRMSE difference under 1% for NEMOH and under 5% for HAMS. This proves that the results are gaining independence from mesh size after a mesh intensity and become almost constant, ignoring numerical errors. All of the results except A and Fe in the heave axis and Fe in the pitch axis are converged in NEMOH faster than in HAMS. Yet, this is just proof of precision, not proof of high accuracy. The accuracy comparisons of the codes are discussed in the next section.

ISSN: 1300-1973, e-ISSN: 2651-530X, Dergi ana sayfası: http://www.gmoshipmar.org/
Araştırma Makalesi

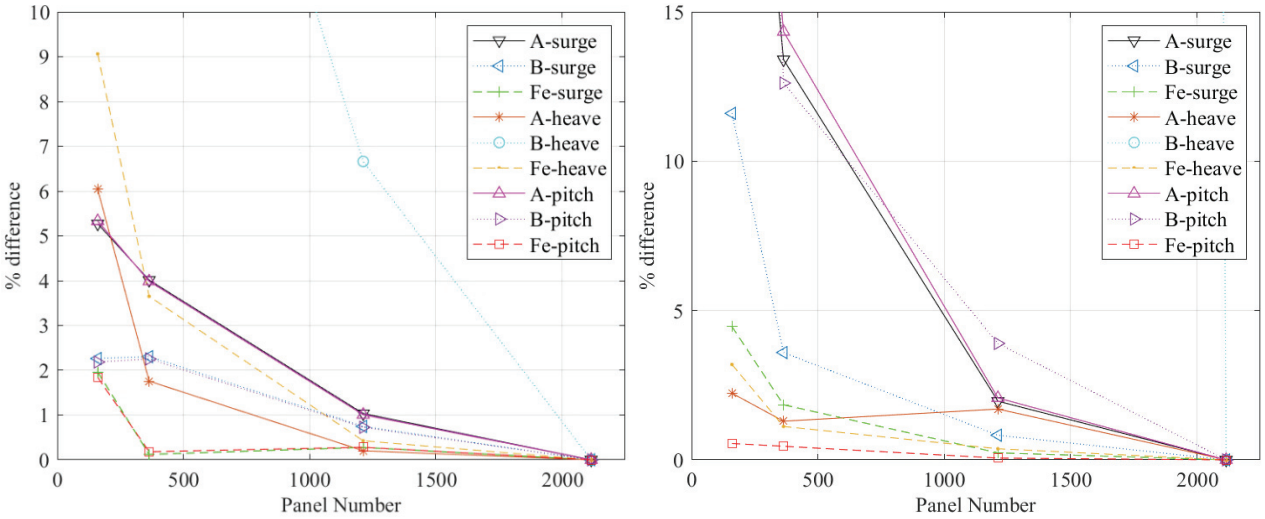

Figure 5. Variation of NRMSE values with panel number for Spar Buoy platform in NEMOH and HAMS

It is noticeable at first glance how close the m3_OC4_Semisub (792 panels) and m4_OC4_Semisub (1314 panel) results are to each other. Contrary to the graph, the independence is not disturbed by the last mesh because the difference between m4_OC4_Semisub and the last mesh is due to the presence of bracings as mentioned previously. Similar to the OC3 Spar Buoy platform, the overall worst convergence results are obtained in the heave axis in radiation damping. Moreover, the subsequent poor convergence results also belong to radiation damping, however, this does not mean the final mesh is inadequate. The compatibility of the radiation damping results for each axis is shown in Figure 6, the pitch axis (B55) in NEMOH is an exception. Comparing the OC3 Spar Buoy platform results with OC4 DeepCWind Semisubmersible, the former has a faster convergence for both potential flow solvers, but the latter has higher precision for NEMOH. The differences are simply due to the complex geometry of the semisubmersible platform.

5. Comparison of BEM solvers

In this study, 0-degree incident wave results of the open-source potential flow solvers NEMOH and HAMS are compared with WAMIT, the most widely accepted and used commercial code. The wider properties of the three BEM solvers are stated in section 2.2. The flexibility and user-friendliness properties of the solvers can be summarized as follows. While WAMIT is the most widely used and accepted code which has an extensive user guide, NEMOH is a widely used open-source code with a user forum with a limited number of users, HAMS is a currently released open-source code needing verification and the code is sparsely documented (Penalba et al., 2017). Although the open-source codes only offer low-order geometry discretization, WAMIT also offers more capable high-order geometry discretization. With a panel limitation of 2000, NEMOH also includes a limited mesh generator, while the remaining codes do not. WAMIT and HAMS are capable of irregular frequency removal and two symmetry plane option, whereas NEMOH cannot. WAMIT generates non-dimensional results, whereas the equivalent information input is simpler in the open-source codes. Although WAMIT enables to use of multiple cores with a parameter in the config.wam and the HAMS enables to determine the number of threads for OpenMP, NEMOH needs source code modification for parallel processing.

GMO Journal of Ship and Marine Technology
Issue: 221, June 2022
ISSN: 1300-1973, e-ISSN: 2651-530X, Journal homepage: http://www.gmoshipmar.org/
Research Article

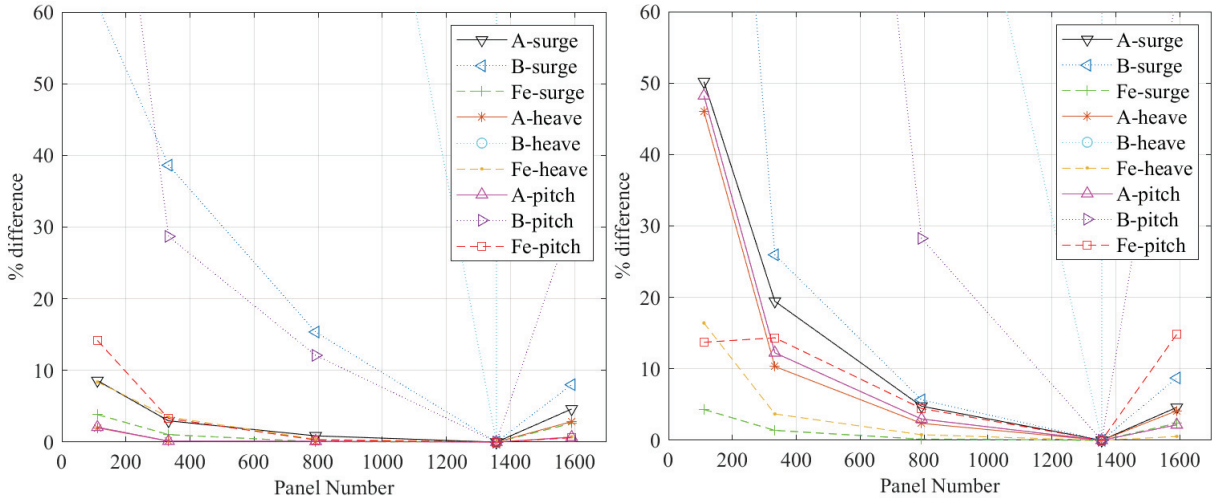

Figure 6. Variation of NRMSE values with panel number for Semisubmersible platform in NEMOH and HAMS

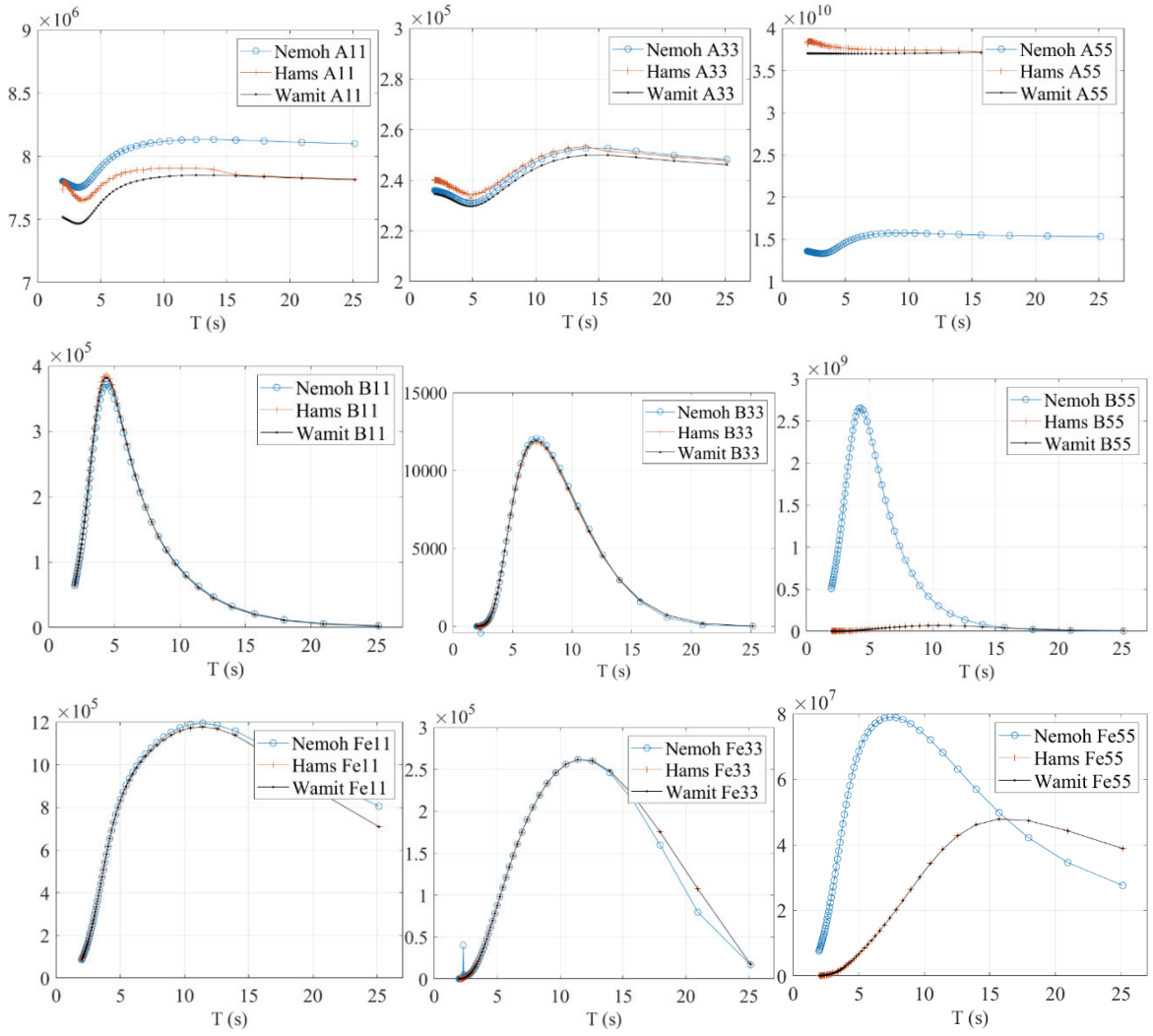

Figure 7. All of the results of OC3 Hywind Spar platform for comparison, units are Ns^2/m for Added Mass, Ns/m for Radiation Damping, and N/m for Excitation Force

A comparison of the codes for the OC3 Hywind Spar-Buoy platform is shown in Figure 7. The results of HAMS are close and tend to be parallel to the WAMIT results with some spikes and steps. Both the

ISSN: 1300-1973, e-ISSN: 2651-530X, Dergi ana sayfası: http://www.gmoshipmar.org/
Araştırma Makalesi

spikes and steps always tend to approach the WAMIT results. On the other hand, the results of NEMOH are almost parallel to WAMIT results with permissible offset, except in pitch. The mesh study revealed that the irrelevant pitch results of NEMOH do not depend on mesh, which is converged and precise. For HAMS, the minimum and maximum NRMS values of added masses are 2.02% in heave and 2.60% in pitch, radiation damping is 1.07% in surge and 47.90% in heave, Excitation force is 1.58% in surge and 20.37% in heave consecutively. Axis-based mean (of A, B, Fe) NRMS values are as follows 1.72% in the surge, 23.43% in heave, and 4.85% in pitch. The statistics reveal that the results of HAMS are adequately close to WAMIT just except for the radiation damping and excitation force in the heave axis. Regarding pitch axis results, beyond the relevant distant results of NEMOH, HAMS itself gave reasonably close results. Ignoring pitch axis results for radiation damping and excitation force, the RMS values of added masses are 3.73% in the surge, 0.70% in heave, and 61.70% in the pitch axis, radiation damping is 5.02% in surge and 355.22% in heave axis, excitation force are 2.67% in surge and 363.65% in heave axis for NEMOH. Both open-source potential flow solvers gave the best results in the surge axis and added mass values overall.

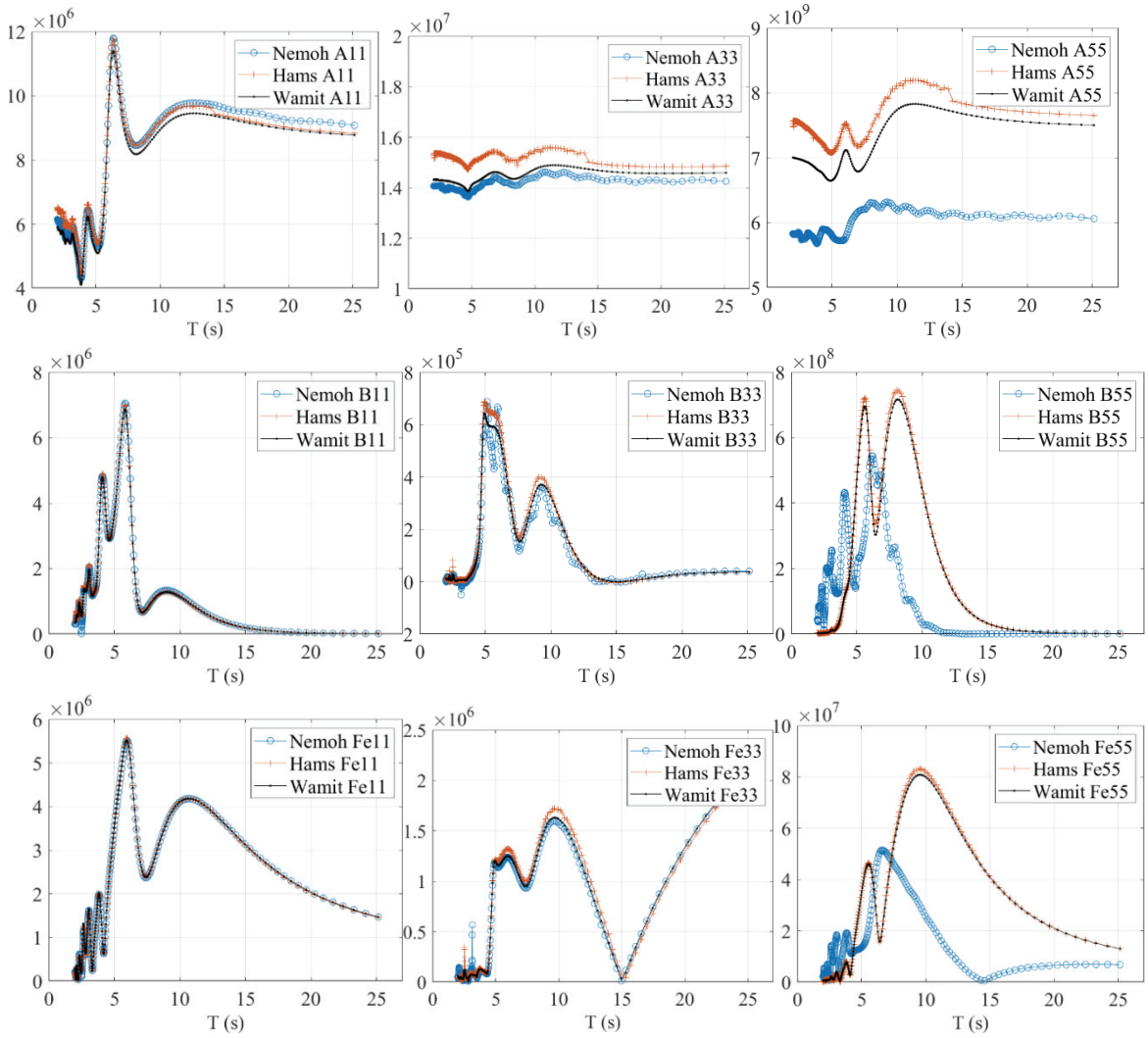

Figure 8. All of the results of OC4 DeepCWind Semisubmersible platform for comparison, units are Ns^2/m for Added Mass, Ns/m for Radiation Damping, and N/m for Excitation Force

Similar to the OC3 Hywind Spar platform, fairly close and mostly parallel results are obtained from HAMS with some spikes and steps, from the OC4 DeepCWind semisubmersible platform as shown in

Figure 8. Not the spikes but the steps mostly approach the WAMIT results but the overall performance of the code is worse than the performance in the case of spar buoy platform due to increased complexity of the hull form. Especially the result of radiation damping in the heave axis is not permissible, which is consistent with the outputs of Andersson (Andersson, 2018). The results of NEMOH tend to follow the same trend as WAMIT despite several fluctuations. The problem of miscalculation of pitch axis values is also observed in this more complex case. While each NRMS value of the HAMS is worse than the spar platform results, the results of NEMOH are better in the heave and pitch axis. Still the results of NEMOH in the pitch axis are far from WAMIT results. For HAMS, the minimum and maximum NRMS values of added masses are 6.31% in heave and 7.65% in the surge, radiation damping is 5.17% in surge and 751.41% in heave, Excitation force are 16.63% in surge and 88.03% in heave consecutively. Axis-based mean (of A, B, Fe) NRMS values are as follows 9.82% in the surge, 281.91% in heave, and 14.59% in pitch for HAMS. Ignoring pitch axis results for radiation damping and excitation force, the NRMS values of added masses are 3.86% in the surge, 1.90% in heave, and 16.35% in the pitch axis, radiation damping is 12.79% in surge and 172.18% in heave axis, excitation force are 29.79% in surge and 85.36% in heave axis for NEMOH. Best results are obtained from both open-source potential flow solvers from surge axis and added mass values, and the most problematic results are obtained from radiation damping overall as in the case of Penalba et al. (2017).

6. Conclusions

In this study, a comparison study was conducted regarding the reliability of open-source panel method codes, based on the solution of two floating wind turbine platforms with a commercial code called WAMIT. NEMOH is the world's first open-source BEM code released in 2014 and is widely used. HAMS is a recently released (Liu, 2019; Liu, 2021) open-source BEM code and both codes need to be verified by comparison. HAMS and NEMOH were compared with WAMIT results and compared with each other on computational performance, flexibility, and user-friendliness. The WAMIT data for the OC3 Hywind Spar and OC4 DeepCWind semi-submersible solutions were taken from previous publications as the basis for this study. These reference values were compared with NEMOH and HAMS for added mass values, potential damping and wave excitation forces. The main purpose of the study is to help researchers select a reliable open-source code as an alternative to approved commercial codes for predicting the hydrodynamic behaviour of offshore structures.

The mesh independence study is represented to show the precision of the codes on their own. To conduct the mesh independence study, four different sized meshes are compared. Rapid convergence is observed for both of the potential flow solvers. The finest meshes of both floating designs have a normalized volumetric representation ratio of about 99%. As expected, the solution time per panel increased as the number of panels increased. Normalized root mean square (RMS) values were utilized for evaluation. Parallel processing was utilized by default in HAMS, but not in NEMOH due to the need for modification in source codes. Even using parallel processing, HAMS was slower than NEMOH. Comparing the mesh convergence, NEMOH showed a faster reaction.

Both of the open-source potential flow codes were quite successful in the simple single-piece spar buoy concept rather than a multibody semisubmersible through NRMS values. The most favourable results were obtained from the surge axis for added mass and the most unfavourable results were obtained from radiation damping in the heave axis. NEMOH gave inappropriate results in the pitch axis for both of the platforms. Neglecting the pitch axis results of NEMOH, both of the codes yielded parallel and reasonably close results to WAMIT.

ISSN: 1300-1973, e-ISSN: 2651-530X, Dergi ana sayfası: http://www.gmoshipmar.org/
Araştırma Makalesi

Further studies are needed to be conducted for different incident wave angles to assess the solution successes of the open-source BEM codes for angle dependencies. The improper solutions of NEMOH in the pitch axis should be improved.

7. References

Andersen, M., Hindhede, D. & Lauridsen, J. Influence of Model Simplifications Excitation Force. Surge for a Floating Foundation for Offshore Wind Turbines. Energies, 8, 2015.

Andersson, E. Application of the open-source code Nemoh for modelling of added mass and damping in ship motion simulations. MS Thesis KTH Royal Institute of Technology Stockholm, Sweden, 2018.

Antonutti, R., Peyrard, C., Johanning, L., Incecik, A. & Ingram, D. The effects of wind-induced inclination on the dynamics of semi-submersible floating wind turbines in the time domain. Renewable Energy, 88, 2016.

Armesto, J. A. et al. Numerical and Experimental Study of a Multi-Use Platform. Volume 6: Ocean Space Utilization; Ocean Renewable Energy, American Society of Mechanical Engineers, 2016. Doi: 10.1115/OMAE2016-54427.

Babarit, A. & Delhommeau, G. Theoretical and numerical aspects of the open source BEM solver NEMOH. 11th European Wave and Tidal Energy Conference (EWTEC2015), Nantes, France, 2015.

Bergdahl, L. Wave-Induced Loads and Ship Motions. MS Thesis Chalmers University of Technology G6teborg, Sweden, 2009.

Bhinder, M. A. & Murphy, J. Evaluation of the Viscous Drag for a Domed Cylindrical Moored Wave Energy Converter. Marine Science and Engineering, 7, 2019.

Bhinder, M. A., Babarit, A., Gentaz, L. & Ferrant, P. Potential time-domain model with viscous correction and CFD analysis of a generic surging floating wave energy converter. International Journal of Marine Energy, 10, 2015.

Butterfield, S., Musial, W. & Jonkman, J. Overview of Offshore Wind Technology. Chinese Renewable Energy Industry Association Wind Power Shanghai Conference, 2007.

Butterfield, S., Musial, W., Jonkman, J. & Sclavounos, P. Engineering Challenges for Floating Offshore Wind Turbines. Copenhagen Offshore Wind Conference, 2007.

Campos, A., Molins, C., Gironella, X. & Trubat, P. Spar concrete monolithic design for offshore wind turbines. Proceedings of the Institution of Civil Engineers - Maritime Engineering, 169, 2016.

Chakrabarti, S. K. Hydrodynamics of offshore structures: Mathematical theory and its applications in structures. Springer-Verlag New York Inc., New York, NY, 1987.

Combourieu, A., Philippe, M., Rongère, F. & Babarit, A. InWave: A New Flexible Design Tool Dedicated to Wave Energy Converters. Volume 9B: Ocean Renewable Energy, American Society of Mechanical Engineers, 2014. Doi: 10.1115/OMAE2014-24564.

Cordle, A. & Jonkman, J. State of the Art in Floating Wind Turbine Design Tools. 21st International Offshore and Polar Engineering Conference, 2011.

Doss, A. Impact of box type floating breakwater on motion response of hydrodynamically coupled floating platforms downstream. MS Thesis Delft University of Technology Delft, Netherlands, 2020.

E. Uzunoglu and C. Guedes Soares, "Hydrodynamic design of a free-float capable tension leg platform for a 10 MW wind turbine," Ocean Engineering, vol. 197, Feb. 2020. Doi: 10.1016/j.oceaneng.2019.106888.

Fang, H. & Duan, M. The Environment and Environmental Load of Offshore Oil Engineering. Offshore Operation Facilities, Elsevier, 2014. Doi:10.1016/B978-0-12-396977-4.00001-9.

Fernandez, G. V., Balitsky, P., Stratigaki, V. & Troch, P. Coupling Methodology for Studying the Far Field Effects of Wave Energy Converter Arrays over a Varying Bathymetry. Energies, 11(11), 2899, 2018. Doi: 10.3390/en11112899.

Fitzgerald, C. J. Nonlinear Potential Flow Models. Numerical Modelling of Wave Energy Converters, Elsevier, 2016. Doi:10.1016/B978-0-12-803210-7.00005-0.

Gonzalez Jimenez, M. A hydrodynamic analysis of three floating offshore wind-wave energy converters differing in the floating stability principle. MS Thesis Delft University of Technology Delft, Netherlands, 2020.

Henderson, A. R. et al. Feasibility Study of Floating Windfarms in Shallow Offshore Sites. Wind Engineering, 27, 2003.

Heronemus, W., E. Pollution-Free Energy from Offshore Winds. 8th Annual Conference and Exposition Marine Technology Society, 1972.

Hughes, J., Williams, A. & Masters, I. A blind test on floats in extreme waves using a transient potential flow model. Proceedings of the Institution of Civil Engineers - Engineering and Computational Mechanics 173, 2020.

IRENA. Renewable Energy Technologies: Cost Analysis Series, 2012. Accessed on 05.20.2021 [Online]. Available: https://www.irena.org/-/media/Files/IRENA/Agency/Publication/2012/RE_Technologies_Cost_Analysis-WIND_POWER.pdf.

Jafaryeganeh, H., Rodrigues, J. M. & Guedes Soares, C. Influence of mesh refinement on the motions predicted by a panel code. Maritime Technology and Engineering (ed. Guedes Soares, C.) Taylor & Francis Group, 2014.

Jonkman, J. & Buhl, M. FAST User's Guide. NREL/TP-500-38230, 2005.

Jonkman, J. & Musial, W. Offshore Code Comparison Collaboration (OC3) for IEA Wind Task 23 Offshore Wind Technology and Deployment. NREL/TP-5000-48191, 2010. Doi: 10.2172/1004009.

Jonkman, J. Definition of the Floating System for Phase IV of OC3. NREL/TP-500-47535, 2010. Doi: 10.2172/979456.

Kim, Y. & Kim, J.-H. Benchmark study on motions and loads of a 6750-TEU containership. Ocean Engineering, 119, 2016.

Ko, K. H., Park, T., Kim, K. H., Kim, Y. & Yoon, D. H. Development of panel generation system for seakeeping analysis. CAD Computer-Aided Design, 43, 848–862, 2011.

Kohlmann, L. A frequency-dependent drag coefficient on the motion response of a hybrid STC wind-wave energy converter. 2019.

Lawson, M., Yu, Y., Ruehl, K. & Michelen, C. IMPROVING AND VALIDATING THE WEC--SIM WAVE ENERGY CONVERTER MODELING CODE. 3rd Marine Energy Technology Symposium, 2015.

Lee, K. Responses of floating wind turbines to wind and wave excitation. MS Thesis Massachusetts Institute of Technology, Dept. of Ocean Engineering, 2005.

Leroy, V., Gilloteaux, J.-C., Philippe, M., Babarit, A. & Ferrant, P. Development of a Simulation Tool Coupling Hydrodynamics and Unsteady Aerodynamics to Study Floating Wind Turbines. Volume 10: Ocean Renewable Energy, American Society of Mechanical Engineers, 2017. Doi: 10.1115/OMAE2017-61203.

Lin, Y. H., Kao, S. H. & Yang, C. H. Investigation of Hydrodynamic Forces for Floating Offshore Wind Turbines on Spar Buoys and Tension Leg Platforms with the Mooring Systems in Waves. Applied Sciences, 9, 608, 2019. Doi: 10.3390/app9030608

Liu, Y. A brief manual for running HAMS. Accessed on 05.28.2021 [online] Available: https://github.com/YingyiLiu/HAMS/tree/master/Manual.

Liu, Y. et al. A reliable open-source package for performance evaluation of floating renewable energy systems in coastal and offshore regions. Energy Conversion and Management, 174, 516–536, 2018.
Liu, Y. HAMS: A Frequency-Domain Pre-processor for Wave-Structure Interactions—Theory, Development, and Application. Marine Science and Engineering, 7, 2019.

Matha, D., Schlipf, M., Cordle, A., Pereira, R. & Jonkman, J. Challenges in Simulation of Aerodynamics, Hydrodynamics, and Mooring-Line Dynamics of Floating Offshore Wind Turbines. 21st Offshore and Polar Engineering Conference Maui, Hawaii, 2011.

Morison, J. R., Johnson, J. W. & Schaaf, S. A. The Force Exerted by Surface Waves on Piles. Petroleum Technology, 2, 1950.

Murray, J. & Barone, M. The Development of CACTUS, a Wind and Marine Turbine Performance Simulation Code. 49th AIAA Aerospace Sciences Meeting including the New Horizons Forum and Aerospace Exposition, American Institute of Aeronautics and Astronautics, 2011. Doi:10.2514/6.2011-147.

Musial, W., Butterfield, S. & Boone, A. Feasibility of Floating Platform Systems for Wind Turbines. 42nd AIAA Aerospace Sciences Meeting and Exhibit, American Institute of Aeronautics and Astronautics, 2004. Doi:10.2514/6.2004-1007.

Olondriz, J., Elorza, I., Trojaola, I., Pujana, A. & Landaluze, J. On the effects of basic platform design characteristics on floating offshore wind turbine control and their mitigation. Journal of Physics: Conference Series, 753, 2016.

Parisella, G. & Gourlay, T. Comparison of open-source code Nemoh with Wamit for cargo ship motions in shallow water. 2016-23, CMST, Curtin University, 2016.

Patel, M. H. Offshore engineering. Mechanical Engineer's Reference Book, Elsevier, 1994. Doi:10.1016/B978-0-7506-1195-4.50018-X.

Penalba, M., Kelly, T. & Ringwood, J. Using NEMOH for Modelling Wave Energy Converters: A Comparative Study with WAMIT. 12th European Wave and Tidal Energy Conference Cork, Ireland, 2017.

Robertson, A. et al. Offshore Code Comparison Collaboration Continuation within IEA Wind Task 30: Phase II Results Regarding a Floating Semisubmersible Wind System. Volume 9B: Ocean Renewable Energy, American Society of Mechanical Engineers, 2014. Doi: 10.1115/OMAE2014-24040.

Robertson, A. N. et al. OC5 Project Phase II: Validation of Global Loads of the DeepCwind Floating Semisubmersible Wind Turbine. Energy Procedia, 137, 2017.

Roessling, A. & Ringwood, J. Finite order approximations to radiation forces for wave energy applications. 1st International Conference on Renewable Energies Offshore, 6771, 2014.

Schubert, B. W., Robertson, W. S. P., Cazzolato, B. S. & Ghayesh, M. H. Linear and nonlinear hydrodynamic models for dynamics of a submerged point absorber wave energy converter. Ocean Engineering, 197, 106828. 2020.

Sclavounos, P., Tracy, C. & Lee, S. Floating Offshore Wind Turbines: Responses in a Seastate Pareto Optimal Designs and Economic Assessment. Volume 6: Nick Newman Symposium on Marine Hydrodynamics; Yoshida and Maeda Special Symposium on Ocean Space Utilization; Special Symposium on Offshore Renewable Energy, ASMEDC, 2008. Doi: 10.1115/OMAE2008-57056.

Shin, H., Kim, B., Dam, P. T. & Jung, K. Motion of OC4 5MW Semi-Submersible Offshore Wind Turbine in Irregular Waves. Volume 8: Ocean Renewable Energy, American Society of Mechanical Engineers, 2013. Doi: 10.1115/OMAE2013-10463.

Uzunoglu, E. & Guedes Soares, C. Hydrodynamic design of a free-float capable tension leg platform for a 10 MW wind turbine. Ocean Engineering, 197, 2020.

Uzunoglu, E. & Soares, C. Influence of bracings on the hydrodynamic modelling of a semi-submersible offshore wind turbine platform. Renewable Energies Offshore, CRC Press, 2015. Doi: 10.1201/b18973-106.

Uzunoglu. E., & Guedes Soares C. A system for the hydrodynamic design of tension leg platforms of floating wind turbines. Ocean Engineering, vol. 171, pp. 78–92, 2019. Doi: 10.1016/J.OCEANENG.2018.10.052.

van der Tempel, J., Diepeveen, N. F. B., de Vries, W. E. & Cerda Salzmann, D. Offshore environmental loads and wind turbine design: impact of wind, wave, currents and ice. Wind Energy Systems, Elsevier, 2011. Doi:10.1533/9780857090638.4.463.

Verbrugghe, T. et al. A Comparison Study of a Generic Coupling Methodology for Modelling Wake Effects of Wave Energy Converter Arrays. Energies, 10(11), 1697, 2017. Doi: 10.3390/en10111697.

Vijay, K. G., Karmakar, D., Uzunoglu, E. & Guedes Soares, C. Performance of barge-type floaters for floating wind turbine. Progress in Renewable Energies Offshore (ed. Guedes Soares, C.) CRC Press, 2016. Doi: 10.1201/9781315229256.

WAMIT Inc. WAMIT User Manual, V7.4, 2006.

Wang, W., Kamath, A., Martin, T., Pákozdi, C. & Bihs, H. A Comparison of Different Wave Modelling Techniques in an Open-Source Hydrodynamic Framework. Marine Science and Engineering, 8, 2020.

ISSN: 1300-1973, e-ISSN: 2651-530X, Dergi ana sayfası: http://www.gmoshipmar.org/
Araştırma Makalesi

Wayman, E. N., Sclavounos, P. D., Butterfield, S., Jonkman, J. & Musial, W. Coupled Dynamic Modelling of Floating Wind Turbine Systems. Offshore Technology Conference, Offshore Technology Conference, 2006. Doi: 10.4043/18287-MS.

Zhao, D., Han, N., Goh, E., Cater, J. & Reinecke, A. Offshore wind turbine aerodynamics modelling and measurements. Wind Turbines and Aerodynamics Energy Harvesters, Elsevier, 2019. Doi:10.1016/B978-0-12-817135-6.00005-3.

Zhou et al. Numerical Modelling of Dynamic Responses of a Floating Offshore Wind Turbine Subject to Focused Waves. Energies, 12, 2019.